

Fabrication and characterization of dual phase magnesia–zirconia ceramics doped with plutonia

P.G. Medvedev^{*}, J.F. Jue, S.M. Frank, M.K. Meyer

Idaho National Laboratory, P.O. Box 1625 Idaho Falls, ID 83415-6160, United States

Abstract

Dual phase magnesia–zirconia ceramics doped with plutonia are being studied as an inert matrix fuel (IMF) for light water reactors. The motivation of this work is to develop an IMF with a thermal conductivity superior to that of the fuels based on yttria stabilized zirconia. The concept uses the MgO phase as an efficient heat conductor to increase thermal conductivity of the composite. In this paper ceramic fabrication and characterization by scanning electron microscopy, energy and wavelength dispersive X-ray spectroscopy is discussed. Characterization shows that the ceramics consist of the two-phase matrix and PuO₂-rich inclusions. The matrix is comprised of pure MgO phase and MgO–ZrO₂–PuO₂ solid solution. The PuO₂-rich inclusion contained dissolved MgO and ZrO₂.

Published by Elsevier B.V.

PACS: 28.41.Bm; 81.05.Je; 81.05.Mh; 28.41.Kw

1. Introduction

Advanced fuel cycle initiative (AFCI) is being pursued by the United States Department of Energy with a four-prong objective: recovery of energy from spent nuclear fuel (SNF), reduction of the inventory of civilian plutonium, reduction of the toxicity and heat load of stored SNF, and more effective use of the SNF repository. AFCI's mission is to develop and demonstrate technologies that enable the transition to a stable, long-term, environmentally, economically and politically acceptable fuel cycle.

Use of existing light water reactors (LWR) as a neutron source to fission plutonium and transmute minor actinides provides a near term opportunity for very effective in-reactor disposition of these surplus nuclear materials [1]. A need for a non-fertile matrix material that can be safely used in LWR fuels as plutonium and minor actinide dilutant drives material development research in this field.

Yttria stabilized zirconia (YSZ) is the most evolved candidate for use in IMF. Both steady-state [2] and transient [3] irradiations of YSZ-based IMF have been performed. Material properties of YSZ have been closely examined [4,5]. Out-of pile irradiation studies designed to understand the mechanism of radiation damage have been completed [6]. Neutronic feasibility of YSZ-based IMF has been also assessed

^{*} Corresponding author. Tel.: +1 208 533 7199; fax: +1 208 533 7863.

E-mail address: pavel.medvedev@inl.gov (P.G. Medvedev).

[7] complemented by core burnup calculations and accident analyses [8]. Despite its excellent radiation resistance, compatibility with reactor materials and good neutronic properties, low thermal conductivity is the main disadvantage of YSZ. According to a recent analysis [7] fuel centerline temperature of the YSZ-based IMF may be 100 K higher than the limit specified for LWRs. Safe use of YSZ as a matrix in LWR fuel is only possible if a reactor is operated at a lower power or if fuel pellets feature central voids. Both measures increase the cost and decrease the feasibility of plutonium disposition.

Use of composites containing a phase with a higher thermal conductivity could improve performance characteristics of zirconia-based IMF. Use of MgO as such a phase has been proposed [9,10]. It has been shown [10] that dual phase MgO–ZrO₂ ceramics have the thermal conductivity superior to that of UO₂ and have notable resistance to the water at the temperature of 573 K and pressure 8.6 MPa, making them attractive for use as an IMF matrix. Development of IMF based on MgO–ZrO₂ ceramics continues at Idaho National Laboratory with the support of the AFCI. The present paper describes results of the first experiment to fabricate dual phase magnesia–zirconia ceramics doped with plutonia as a potential IMF form for use in LWRs.

2. Fabrication

Dual phase magnesia–zirconia ceramics doped with plutonia were fabricated from the oxide powder mixture using conventional pressing and sintering techniques. The fabrication process was based on the earlier work [10] that dealt with non-radioactive materials. The flow diagram of the fabrication process is shown in Fig. 1.

Pre-weighed amounts of magnesia and magnesium zirconium oxide powders were combined with water in a beaker. The weight of water was approximately three times greater than the weight of the powders combined. The water and powder mixture was stirred using a magnetic stirring bar for 6 h. The slurry was dried in air at 353 K for 5 h. The resulting powder was transferred into an alumina crucible and heat-treated at 1273 K for 5 h in a high temperature tube furnace. The ramp-up and ramp-down rates were 10 K min⁻¹. Upon cool-down, zinc stearate (Fisher Scientific Fair Lawn, NJ Z-78-4, lot 871095, UPS grade) in the amount of 1% by weight was mixed into the powder using a mortar and a pestle.

The powder was then pressed into pellets with a force of 13.34 kN using a cylindrical die of 12.72 mm diameter. Resulting MgO–ZrO₂ pellets weighing 3.8986 g and 3.3571 g were transferred into a glovebox. Once in the glovebox, the pellets were ground and 1.0265 g of PuO₂ powder was mixed in using a mortar and pestle. The powder was then pressed into pellets with a force of 44.45 kN using a cylindrical die of 12.72 mm diameter. Resulting pellets were ground into powder using a mortar and pestle. The powder was passed through a sieve with an aperture size of 250 μm. The mixture was pressed again into pellets with a force of 13.34 kN using a cylindrical die of 12.72 mm diameter. The pellets were placed into an alumina crucible and sintered in air for 7.5 h at 1973 K in a high temperature box furnace. The ramp-up rate was 10 K min⁻¹ up to 1273 and 5 K min⁻¹ from 1273 to 1973 K. The ramp-down rate was 10 K min⁻¹. The pellets were cooled in the furnace after sintering.

Magnesium oxide was procured from Cerac Incorporated (Milwaukee, WI, item M-1017, lot X25111, typically 99.95% pure). Magnesium zirconium oxide supplied by Alfa Aesar (Ward Hill, MA, stock 12343, lot C01E, 99.7% metals basis) was used as a source of zirconia. Use of magnesium zirconium oxide facilitated obtaining a homogeneous distribution of MgO and ZrO₂ in the final product.

3. Characterization of dual phase magnesia–zirconia ceramics doped with plutonia

3.1. Visual inspection, dimensions, weight and density

Two ceramic pellets were fabricated. Photographs of the pellets are shown in Fig. 2. As-sintered pellets are shown in Fig. 2(a). Pellet cross-section exposed by cutting a pellet with a diamond saw is shown in Fig. 2(b). Each pellet featured one crack near one face as illustrated in Fig. 2(c). The crack was probably caused by density gradients developed during pressing.

The pellets were weighed and measured with a caliper. Results of the measurements are shown in Table 1. Pellet diameter was measured three times: in the mid-pellet and near each face. Pellet hourglassing developed during sintering was manifested by diameter decrease in the mid-pellet region.

Pellet density values derived from weight and volume and measured by water immersion technique are included in Table 1. The pellet density was

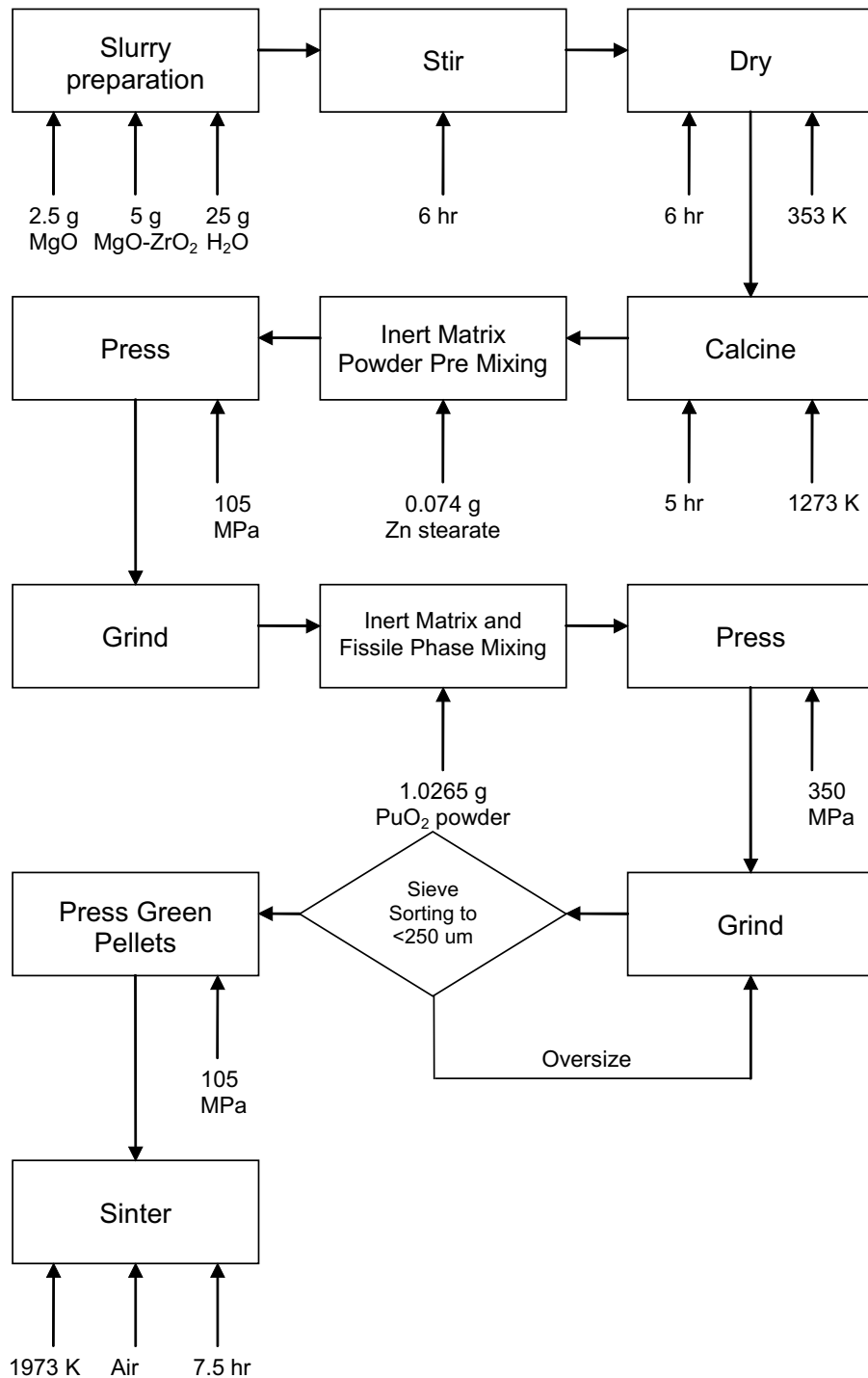


Fig. 1. Flow diagram for fabrication of MgO-ZrO₂-PuO₂ ceramics.

significantly lower than that of MgO-ZrO₂ ceramics studied in the earlier work [10]. MgO-ZrO₂ ceramics containing 50 wt% of MgO had the density of 4.39 g cm⁻³ measured by water immersion.

3.2. Scanning electron microscopy

Scanning electron microscopy (Zeiss DSM960A digital scanning electron microscope), energy and

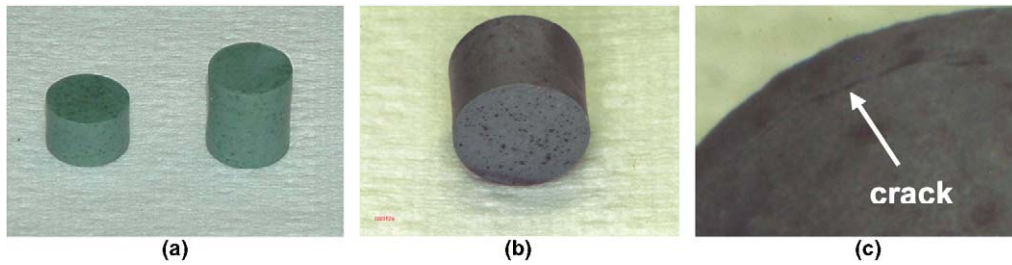


Fig. 2. Fabricated MgO–ZrO₂–PuO₂ ceramic pellets. (a) As-sintered pellets, (b) pellet cross-section, (c) crack near the face of the pellet.

Table 1
Dimensions and weight of the sintered ceramic pellets

Pellet	Weight (g)	Length (mm)	Diameter (mm)				Density (g cm ⁻³)	
			Face	Mid-pellet	Face	Average	Bulk	Immersion
1	5.0406	13.00	11.59	11.40	11.60	11.53	3.71	3.8157
2	2.9043	7.48	11.57	11.42	11.55	11.51	3.73	3.8751

wavelength dispersive X-ray analyses (Oxford Instruments, Fremont, CA) were carried out with an objective to identify the phases present in the ceramics and to determine chemical composition of each phase. Previous fabrication and characterization studies [10] established that MgO–ZrO₂ and MgO–ZrO₂–Er₂O₃ systems containing from 40 to 70 wt% of ZrO₂ and 7 wt% Er₂O₃ sintered in air at 1973 K consisted of two phases: zirconia-based cubic solid solution and pure cubic magnesia. The amount of magnesia dissolved in the zirconia-based cubic solid solution phase was 13–17 mol.%. Erbium dopant preferentially dissolved in the zirconia phase. Presence of pure MgO phase in the ceramics had a positive effect on their thermal conductivity. The same effect is desired in the MgO–ZrO₂–PuO₂ system. Thus, understanding the behavior of PuO₂ dopant in the MgO–ZrO₂ system is of particular importance.

To produce a sample for the scanning electron microscopy (SEM) the pellet was cut with a diamond saw yielding a disk approximately 2 mm thick. The disk was broken up to produce smaller fragments by tapping with a pestle. One of the resulting fragments was mounted in the epoxy and manually polished with the silicon carbide paper of 600, 800, and 1200 grits. The polishing time was kept to a minimum in order to reduce the personnel radiation exposure. The sample submitted for analysis is shown in Fig. 3.

Fig. 4 shows key microstructural features identified in the sample: a two-phase matrix (Fig. 4(a))

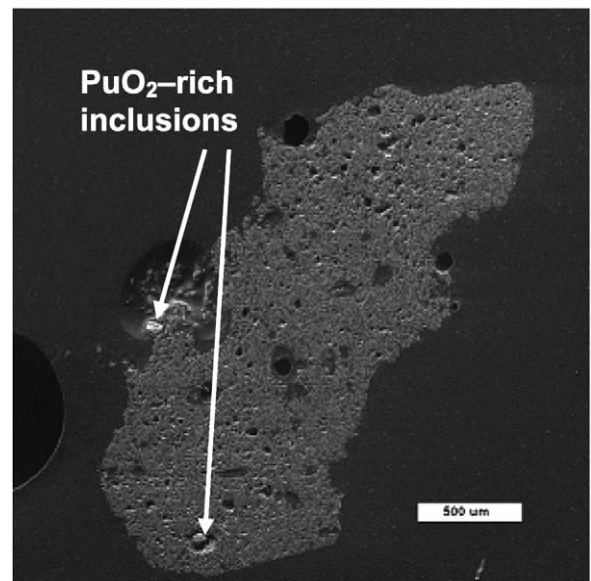


Fig. 3. SEM image of the MgO–ZrO₂–PuO₂ ceramic sample submitted for analysis. The black area surrounding and black shapes within the sample are the mounting epoxy. The sample consists of a matrix and PuO₂-rich inclusions.

and a PuO₂-rich inclusion (Fig. 4(b)). The matrix was found to consist of pure MgO phase (dark phase in Fig. 4(a)) and MgO–ZrO₂–PuO₂ solid solution (light phase in Fig. 4(a)). Except for the greater porosity, the microstructure of the matrix was found to be virtually identical to that observed in MgO–ZrO₂ and MgO–ZrO₂–Er₂O₃ systems [10]. The PuO₂-rich inclusion shown in Fig. 4(b)

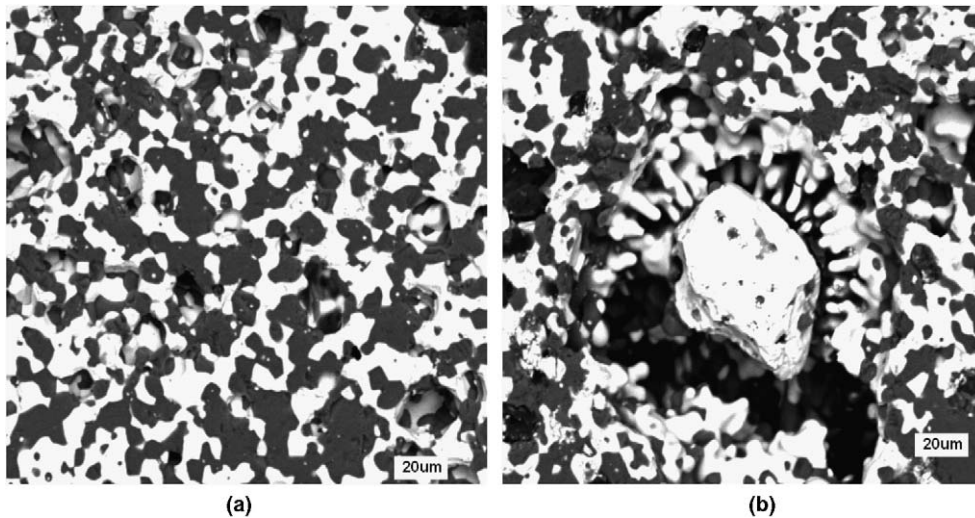


Fig. 4. Key microstructural features identified in the sample are a two-phase matrix (a) and a PuO_2 -rich inclusion (b). The matrix consisted of pure MgO phase (dark phase) and $\text{MgO-ZrO}_2\text{-PuO}_2$ solid solution (light phase). The PuO_2 -rich inclusion contained MgO and ZrO_2 with PuO_2 being a dominant component.

contained MgO and ZrO_2 with PuO_2 being a dominant component. The columnar grains surrounding the PuO_2 -rich inclusion were believed to be formed due to significant variation of ZrO_2 solubility in PuO_2 with temperature. Examination of the PuO_2 -rich end of the $\text{PuO}_2\text{-ZrO}_2$ phase diagram [11] revealed that the solubility of ZrO_2 in PuO_2 increases from 20 to 60 mol.% with the increase of temperature from 1473 to 1973 K. Therefore, this

variation in solubility caused diffusion of ZrO_2 into the PuO_2 particle during the furnace ramp-up and sintering, and rejection of ZrO_2 by PuO_2 -rich particle during furnace ramp-down. Rejection of ZrO_2 by the PuO_2 -rich particle caused particle densification which led to the formation of a gap between the particle and the matrix observed in Fig. 4(b).

Energy dispersive X-ray spectroscopy (EDS) was used to determine chemical composition of the

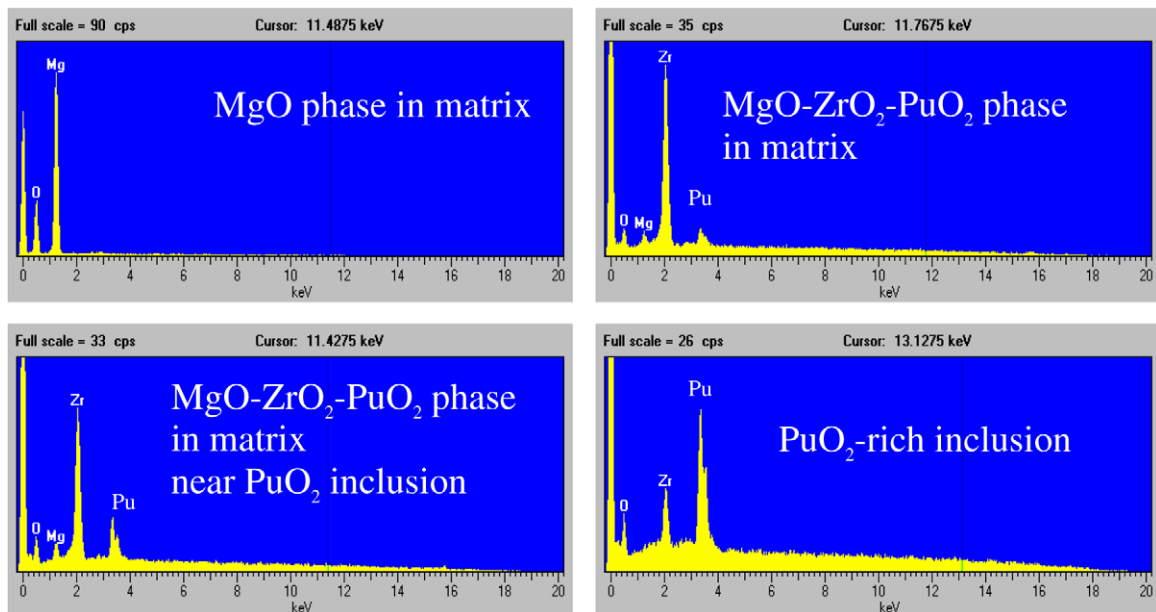


Fig. 5. Typical EDS spectra observed in various locations in the ceramic.

Table 2
Results from SEM EDS semi-quantitative analysis

Phase	Mg (at.%)	Zr (at.%)	O (at.%)	Zr to Mg atomic ratio
MgO grains in matrix	48.29 ± 0.92	0.06 ± 0.04	51.65 ± 0.94	
MgO–ZrO ₂ –PuO ₂ grains in matrix	3.68 ± 0.37	23.19 ± 1.10	73.13 ± 1.00	6.38 ± 0.83
PuO ₂ -rich inclusion	0.91 ± 0.32	9.66 ± 0.64	89.43 ± 0.87	12.63 ± 5.81

Note that the ISIS EDS system cannot perform quantitative analysis for elements heavier than uranium.

phases present in the ceramics. Typical EDS spectra are shown in Fig. 5. As evident from Fig. 5, the matrix Pu content is higher in the vicinity of PuO₂-rich inclusions. This observation suggests that the solubility limit of PuO₂ in the matrix locations away from the inclusions was not reached. Thus, observed undesirable inhomogeneity is possibly due to inadequate mixing rather than the limited solubility of PuO₂ in the matrix.

Detailed EDS results are shown in Table 2. EDS spectra were taken in 15 locations in MgO–ZrO₂–PuO₂ grains, 10 locations in MgO grains, and 5 locations in a PuO₂-rich inclusion. Thus, the numbers in Table 2 are the averages and the standard deviations of these multiple measurements. It should be noted that our EDS system is not capable of quantifying the Pu content. As follows from Table 2, very small amounts of ZrO₂ were detected in the MgO grains. This fact was attributed to the presence of ZrO₂ in the neighboring MgO–ZrO₂–PuO₂ grains and possibly to the contamination of the surface of the MgO grains during polishing. Wavelength dispersive spectroscopy (WDS) did not detect dissolved ZrO₂ and PuO₂ in MgO. Detection limit of WDS was 200 ppm.

4. Conclusions

Dual phase magnesia–zirconia ceramics doped with plutonia were fabricated and characterized by SEM, EDS and WDS. Ceramics were found to consist of the two-phase matrix and PuO₂-rich inclusions. The matrix was comprised of pure MgO phase and MgO–ZrO₂–PuO₂ solid solution. The PuO₂-rich inclusion contained dissolved MgO and ZrO₂. Based on the characterization work it was

concluded that the fabrication process must be modified to achieve homogeneity of the product, reduce porosity, and produce an acceptable fuel form. Improved mixing and calcination of PuO₂ powder together with MgO and ZrO₂ will be utilized during fabrication of the next batch of the ceramics.

The results of this study provide valuable insight on the phase relations in the MgO–ZrO₂–PuO₂ system. The study established that neither PuO₂ nor ZrO₂ dissolved in the highly thermally conductive MgO phase. By remaining free from dissolved species, the MgO phase is expected to maintain its high thermal conductivity acting as efficient means of increasing the thermal conductivity of the entire ceramic composite.

References

- [1] C. Degueldre, U. Kasemeyer, F. Botta, G. Ledergerber, *Mater. Res. Soc. Symp. Proc.* 412 (1996) 15.
- [2] Ch. Hellwig, U. Kasemeyer, *J. Nucl. Mater.* 319 (2003) 87.
- [3] T. Nakamura, H. Sasajima, T. Yamashita, H. Uetsuka, *J. Nucl. Mater.* 319 (2003) 95.
- [4] C. Degueldre, J. Paratte, *Nucl. Technol.* 123 (1998) 21.
- [5] C. Degueldre, T. Arima, Y.W. Lee, *J. Nucl. Mater.* 319 (2003) 6.
- [6] K. Yasuda, C. Kinoshita, S. Matsumura, A.I. Ryazanov, *J. Nucl. Mater.* 319 (2003) 74.
- [7] U. Kasemeyer, Ch. Hellwig, J. Lebenhaft, R. Chawla, *J. Nucl. Mater.* 319 (2003) 142.
- [8] H. Akie, Y. Sugo, R. Okawa, *J. Nucl. Mater.* 319 (2003) 166.
- [9] S. Lutique, R.J.M. Konings, V.V. Rondinella, J. Somers, T. Wiss, *J. Alloys Compd.* 352 (2003) 1.
- [10] P.G. Medvedev, Development of dual-phase magnesia–zirconia ceramics for light water reactor inert matrix fuel, Dissertation, Texas A&M University, 2004.
- [11] P.G. Mardon, D.J. Hodkin, J.T. Dalton, *J. Nucl. Mater.* 32 (1969) 126.